Techno-Science Research Journal V14 (2) (2026) P 50-57

Content list available at ITC

Techno-Science Research Journal

Journal Homepage: http://techno-srj.itc.edu.kh/

Techno-Science Research Journal

# DEM Parameter Calibration of Biomass Materials (Sawdust, Tree Leaves, and Mixture) Using Experimental Angle of Repose Tests

Chantola Chea[1], Kinnaleth Vongchanh[1,2*], Hollin Hoeung[1], Latin Heang[1,2], Sarin Chan[1]

[1] *Thermal lab., Department of Industrial and Mechanical Engineering, Institute of Technology of Cambodia, Russian Federation Blvd., P.O. Box 86, Phnom Penh, Cambodia*

[2] *Research and Innovation Center, Institute of Technology of Cambodia, Russian Federation Blvd., P.O. Box 86, Phnom Penh, Cambodia*

Received: 17 September 2025; Revised: 16 December 2025 Accepted: 11 February 2026; Available online: 31 August 2026

**Abstract:** *The Discrete Element Method (DEM) is widely used to simulate biomass material handling, but accurate simulation requires appropriate parameter calibration. This study calibrated DEM parameters for fibrous and irregular biomass materials, including sawdust (SD), tree leaves (TL), and a 70:30 SD:TL mixture, which exhibit more complex flow behavior than conventional granular materials. A fixed funnel method was employed to measure the static AoR of sawdust (SD), tree leaves (TL), and their mixture. For TL, three material samples (T1-T3) were tested with six repetitions, giving 18 AoR measurements. For SD and the mixture, two samples each (S1-S2 and M1-M2) were tested with six repetitions per sample, yielding 12 measurements per material. The AoR results are reported as mean ± standard deviation were 39.28° ± 0.88° (SD), 41.72° ± 1.70° (TL), and 40.08° ± 1.03° (mixture). DEM simulations (Hertz–Mindlin with JKR cohesion) were tuned by comparing simulated and experimental AoR. Initial parameter sets were defined through literature review and tested in DEM, with the best-fitting parameters identified by comparing simulated AoR with experimental results. The best-fit parameters were as follows (values reported in the order of sawdust, tree leaves, and mixture, respectively): Poisson's ratio (0.300, 0.300, 0.260), shear modulus in MPa (6.000, 10.000, 7.684), restitution coefficient (0.020, 0.002, 0.067), static friction (0.760, 0.600, 0.660), rolling friction (0.120, 0.070, 0.080), and JKR surface energy in J/m$^2$ (0.120, 0.100, 0.098). The relative error between the simulated and experimental AoR was 0.63% for sawdust, 0.15% for tree leaves, and 1.29% for their mixture. These results provide valuable insights for accurately simulating the behavior of biomass materials, such as sawdust and tree leaves, in DEM-based processing systems.*

**Keywords:** Angle of Repose (AoR); Discrete Element Method (DEM); Mixture; Sawdust; Tree leaves

## 1. INTRODUCTION

The shift toward sustainable energy sources has significantly increased interest in biomass utilization, focusing on developing efficient handling and conversion processes [1,2,3]. Biomass is a potential eco-friendly and renewable energy source for the substitution of fossil and solid fuel from forestry. It picks up carbon during growth and releases it after combustion, making it a $CO_2$-neutral energy source [4]. Additionally, it may co-fire with coal, improving energy security and lowering reliance on fossil fuels [5,6]. Briquettes made from biomass waste, such as sawdust and tree leaves, offer a practical solid fuel alternative in addition to aiding with waste management [7]. However, the cohesive structure, uneven particle sizes, and variable moisture content of biomass materials make handling them difficult [8,9]. These elements have an impact on flow behavior; research has shown that systems made for conventional granular materials have problems with compressibility and arching [10,11]. Although mechanical processing can increase flow, it frequently requires more energy [12]. Reducing downtime in industrial operations requires an accurate assessment of whether biomass may cause flow-related issues. Shear testing and other physical characterisation techniques, however, can be labor-intensive [13].

The Discrete Element Method (DEM) has emerged as a useful simulation method to better comprehend and handle these difficulties. This modeling was first created by Cundall and Strack [14] to show the influence of small-scale interactions on the bulk material flow and visualize the

* Corresponding author: Kinnaleth Vongchanh
*E-mail: kinnalethv@itc.edu.kh*

granules' behavior [15]. Recent developments in DEM include simulating irregular particle morphologies [16], capillary forces [17], microcrack buildup [18], and the loss of energy. In the context of industry, DEM has proven particularly helpful in the design and optimization of machinery used in the processing of minerals and biomass [19].

Accurate DEM simulation of biomass is still difficult despite its increasing use, particularly when adjusting characteristics like particle density, stiffness, and friction. Although having a significant impact on outcomes, these criteria are frequently ignored [20]. For accurate findings, calibration is necessary, and there are various techniques available. A three-level validation methodology was presented by Hofmann (2005) [21], which included flow and contact-level calibration in addition to full-scale experiments. By lowering computing complexity while preserving high accuracy, researchers have improved predicted reliability in geotechnical applications by the use of simplified calibration based on bulk density and angle of repose (AoR) for granular material flow DEM modeling [22,23].

Numerous investigations have further shown, employing techniques like the fixed funnel or stacking tests, the efficacy of AoR-based calibration across various materials [24,25]. It has been demonstrated that elements, including surface energy, rolling friction, and the restitution coefficient, have a big impact on AoR outcomes. Calibrated DEM models of tea and sugarcane leaves, for example, showed that precise friction and cohesion parameters may accurately reproduce real-world behavior with little error [26,27].

However, the uneven forms, varying levels of moisture, and natural cohesiveness of biomass materials like sawdust and tree leaves present further barriers for the calibration of DEM. In particular, reliable DEM input parameters for these materials are still limited in the literature. To address this gap, key DEM parameters are calibrated in this study by experimentally determining AoR values using the fixed funnel method. The study aims to experimentally measure and simulate the AoR of tree leaves, sawdust, and their mixture consisting of 70% sawdust and 30% tree leaves by weight, which is optimal for mixing proportion of the briquetting process for these two materials, as reported by Heang et al. (2020) [7]. The resulting calibrated parameters, including friction coefficients, restitution, and surface energy, are to enhance model realism and enable more reliable DEM-based analysis of biomass mixing behavior in subsequent processing simulations.

## 2. METHODOLOGY

### *2.1 Angle of Repose Measurement Methods*

The angle of repose (AoR) is widely used to characterize how granular materials flow, but there's no single standardized way to measure it. According to Rackl et al. (2017) [28], the method must correspond with the purposes of the study and the characteristics of the material. Common AoR techniques include the tilting box, fixed funnel, hollow cylinder, rotating drum, and internal flow funnel, according to Beakawi Al-Hashemi et al. (2018) [24]. The spinning drum measures dynamic AoR from rotating particle motion [29,30], while the hollow cylinder records static AoR during gradual vertical lifting [31]. Each offers distinct insights. When material is discharged, the interior funnel measures the flow [32,33], and the tilting box calculates surface friction, which is sometimes mistaken for AoR [34,35]. While each method has its strengths, many face challenges such as complex setup or limited repeatability. The fixed funnel method, in contrast, offers a simple and reliable approach, especially suitable for cohesive biomass materials. In this method, material is poured from a specific height to form a conical pile, making it an ideal choice for this study due to its ease of use and consistent results [33].

### *2.2 Biomass Materials*

The biomass materials used in this study, sawdust (SD) and tree leaves (TL), were chosen for their relevance to briquette making. Originally, the materials were prepared in a previous study conducted in our laboratory [7], and the same preparation methods were used here. Both materials were air-dried, then mechanically ground and sieved to obtain particles less than 8 mm, which is suitable for feeding into a briquetting machine. After preparation, SD and TL were mixed at a 70:30 mass ratio to create the biomass mixture. The measured bulk densities from the previous work were 230 $kg/m^3$ for SD, 97 $kg/m^3$ for TL, and 163 $kg/m^3$ for the mixture. For the AoR experiment, a 100 g sample consisting of 70 g SD and 30 g TL was used as shown in **Fig. 1**.

a. Sawdust b. Tree leaves

**Fig. 1.** Biomass Materials [7]

### *2.3 Angle of Repose (AoR) Experiment*

The experiment was conducted in accordance with International Standard ISO 4324:1977 [36]. A funnel with a 45 mm outlet was positioned 150 mm above the base, matching the diameter of the collection pad. The angle of repose (AoR) was then determined using Eq. 1, based on the measured height of the resulting conical pile, as illustrated in Fig.2.

$$\phi = \tan^{-1} H/(d/2) \qquad \text{(Eq. 1)}$$

where:

$\phi$ = angle of repose (°)

H = height of the cone (m)

d = diameter of the pad (m)

In parallel, images of the conical heaps were captured and analyzed using ImageJ software [29,37,38]. The images were first converted to binary for edge detection, and the pile slopes were measured using the Angle Tool by fitting linear segments to the heap surface. Multiple angle measurements were taken from each image and averaged to obtain the final AoR. Each material sample consisted of six experimental replicates (Test 1-6) to ensure result consistency and reliability.


(a) (b)

**Fig. 2.** AoR (a) measurement theory (b) experimental setup

*2.4 DEM Simulation*

To simulate the inter-particle behavior of cohesive biomass materials such as SD and TL, the Hertz-Mindlin contact model with JKR bonding was employed [39,40]. Materials having moisture content, fiber structure, or static electricity can all be used with this model [41,42,43]. Static and rolling friction, the restitution coefficient, Young's modulus, and surface energy are important factors that affect flow behavior [44]. To capture van der Waals and capillary forces in moist or cohesive biomaterials, adhesion and cohesion must be described using the JKR framework [45]. A previous study [27] found the rolling friction of tea leaves was 0.067, and static friction was 0.865. Moreover, [26] found the static and rolling friction were 0.21 and 0.05, respectively, for sugarcane leaves, while [46] found the static friction of 0.306 and rolling friction of 0.198 for the same material. Then, [33] calibrated the key parameter of the mixed biomass sawdust was found to be the density of 399.22 kg/m$^3$, with a Poisson's ratio of 0.30, a restitution coefficient of 0.47, and a JKR surface energy of 0.29 J/m², as well as a rolling friction of 0.39. Through the combination of the above studies and the EDEM GEMM database [47], the parameters for SD, TL, and Mixture are compiled in Table 1. These values represent literature-based input ranges and were not calibrated. The ranges were organized into parameter series (A-E for TL, F for SD, and G, H for Mixture) to guide the subsequent AoR calibration.

For the AoR calibration simulations, all DEM models were executed in a virtual box measuring 510 mm × 316 mm. A 3D-designed funnel geometry was imported into EDEM, modeled with material properties [48], including a Poisson's ratio of 0.3, density of 7800 kg/m³, and shear modulus of 7 × 10$^{10}$ Pa. Particle–wall interaction parameters were fixed, such as restitution coefficient = 0.8, static friction = 0.6, and rolling friction = 0.1. Particles were released from a blocked funnel, and simulations were run at a Rayleigh time step of 20% for a total duration of 6 seconds, as shown in Fig. 3. The particle counts were 1946 for SD, 2307 for TL, and 2289 for the mixture. The simulated AoR values were then extracted and analyzed using EDEMPy.

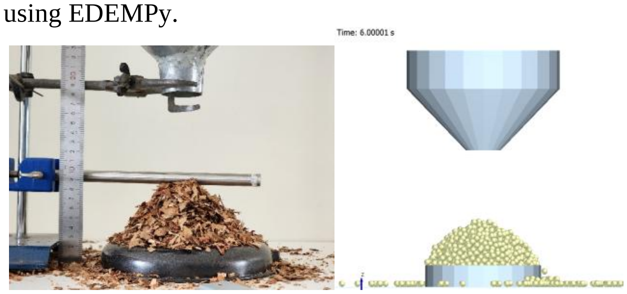


**Fig. 3.** AoR (a) experimental test (b) EDEM simulation

**Table 1.** Range of values of Parameters

| Parameter (between particles) | Sawdust (SD) | Tree leaves (TL) | Mixture (SD+TL) |
|---|---|---|---|
| Poisson's ratio | 0.100-0.500 | 0.1-0.4 | 0.2-0.4 |
| Shear modulus/MPa | 1.000-10 | 1-10 | 1-10 |
| Restitution coefficient | 0.1-0.8 | 0.002-0.005 | 0.050-0.300 |
| Static friction coefficient | 0.01-0.8 | 0.2-0.9 | 0.3-0.8 |
| Rolling friction coefficient | 0.01-0.8 | 0.02-0.07 | 0.03-0.08 |
| JKR surface energy/J/m$^2$ | 0.05-0.5 | 0.1-3.5 | 0-0.2 |

## 3. RESULTS AND DISCUSSION

*3.1 Angle of Repose*

The angle of repose (AoR) was measured under the same conditions for tree leaves (TL), sawdust (SD), and their mixtures. Three TL samples (T1, T2, T3), two samples (S1, S2), and two mixture samples (M1, M2) were tested. Each sample consisted of six experimental replicates (Test 1 to Test 6). Then the results are reported as T1J/T1F, T2J/T2F, and T3J/T3F, where J represents AoR from ImageJ software and F represents AoR calculated by formula.

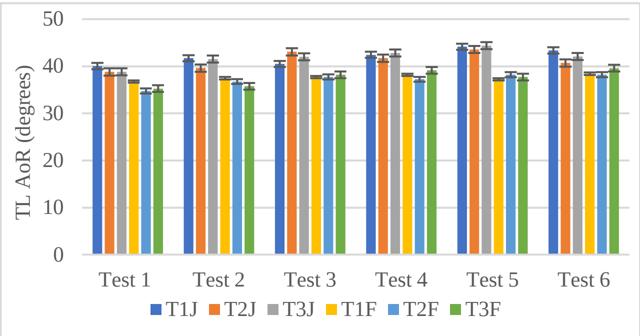


**Fig. 4.** Mean AoR comparison obtained from six repetitions (Test 1-6) for three TL samples (T1, T2, and T3), measured using the ImageJ (J) and formula-based (F) methods

Among the three types of samples, tree leaves showed the most variation in AoR due to their light weight and irregularly flat surface, leading to overlap when settling. When large or rigid leaf fragments populated, steeper slopes formed, increasing interlocking between particles and causing pile resistance to sliding. As compared in Fig.4, the ImageJ approach consistently provided higher values than the formula-based approach, allowing for better detection of finer surface angles, as shown in Test 5, where T1J measured 44.133° using ImageJ compared to 38.190° using the formula.

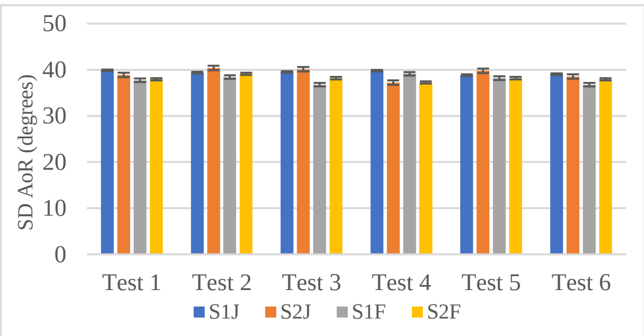


**Fig. 5.** Mean AoR comparison obtained from six repetitions (Test 1-6) for two SD samples (S1 and S2), measured using the ImageJ (J) and formula-based (F) methods

Sawdust, on the other hand, behaved very differently. Its finer, more uniform particles settled into consistent slopes across both sample tests (S1 and S2 are two samples for sawdust). A particle heavier than a tree leaf that easily slides down, creating a smaller steep. As a result, AoR for sawdust stayed within a tight range, typically between 36° and 41°, regardless of which sample was used, as shown in Fig.5. This stability reflects sawdust's relatively predictable flow characteristics.

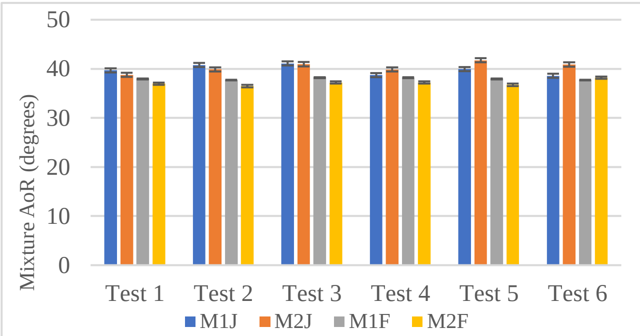


**Fig. 6.** Mean AoR comparison obtained from six repetitions (Test 1-6) for two mixture samples (M1 and M2), measured using the ImageJ (J) and formula-based (F) methods

When the two materials were mixed, the AoR fell in between. The presence of sawdust helped reduce the voids and bridging often seen in leaf-only samples, resulting in smoother piles with moderately steep slopes. From Fig.6, the ImageJ method produced slightly higher values than the AoR calculated by the formula, with a mean difference of 2.53°, indicating its sensitivity to surface contours.

Across all three samples, the ImageJ method consistently produced higher angle of repose (AoR) values than the formula-based approach. The differences were generally small, within 2–4°, but they appeared consistently across tests. This is mainly because ImageJ captures local irregularities of the pile, which are particularly noticeable for non-uniform materials such as tree leaves. By contrast, the formula method assumes the pile is perfectly conical, which reduces variation but oversimplifies the pile shape, leading to lower AoR values.

**Table 2.** Summary of Mean AoR and Standard Deviation (StDev) for SD, TL, and Mixture Using ImageJ and Formula Methods

| Material | Method | Mean AoR (°) | StDev (°) |
|---|---|---|---|
| SD (S1J, S2J) | ImageJ | 39.28 | 0.880 |
| SD (S1F, S2F) | Formula | 37.85 | 0.865 |
| TL (T1J, T2J, T3J) | ImageJ | 41.72 | 1.704 |
| TL(T1F,T2F,T3F) | Formula | 37.45 | 1.257 |
| Mixture (M1J, M2J) | ImageJ | 40.08 | 1.032 |
| Mixture (M1F, M2F) | Formula | 37.55 | 0.592 |

As summarized in Table 2, the ImageJ method reported higher averages (41.72° for tree leaves, 39.38° for sawdust, and 40.08° for the mixture), whereas the formula method yielded consistently lower and narrowly distributed values around 37°. The formula's simplicity limits its accuracy, while ImageJ reflects the true geometry of irregular piles, resulting in slightly larger deviations, especially in materials with uneven surfaces like leaves. This difference range is also reported for pharmaceutical powders, which is between the image processing and the formula within 2° [49], while much larger gaps (10–15°) have been reported for wheat grains [50].

### *3.2 Simulation Parameter Calibration Results*

This study adopted a systematic trial-and-error approach. In contrast, DEM calibration studies often employ statistical or optimization-based methods, such as Design of Experiments (DoE) or Response Surface Methodology (RSM) [25,33]. Despite its simplicity, this method successfully identified parameter sets with close agreement to experimental AoR values, comparable in accuracy to more advanced methods.

Based on the previous research on biomass and fibrous material simulations, initial ranges for key DEM parameters were identified and used to construct a series of trial-and-error calibration sets. For tree leaves, five simulation series (A–E) were conducted. Series A served as the baseline, and its results guided the refinement in Series B. Subsequent series (C, D, and E) were developed iteratively to minimize the relative error between simulated and experimental AoR. This method leads to non-standardization of each set, as listed in Table 3.

**Table 3.** Summary of AoR Results from Initial Parameter Screening – Tree leaves

| Series | Set Count | AoR Range (°) | Closest Match (°) | Notes |
|---|---|---|---|---|
| Series A | 8 | 37–43 | A7 (41.66) | Best baseline for refinement |
| Series B | 13 | 41–47 | B7 (41.99) | Close, but high StDev |
| Series C | 6 | 43–48 | C2 (45.81) | High AoR, not selected |
| Series D | 9 | 46–48 | D2 (46.30) | Too high AoR |
| Series E | 12 | 38–51 | E4 (39.74) | Unstable results |

Table 4 shows that Series A produced A7, which had an AoR (41.66°) closest matching the experimental value. Series B identified B7 with the closest AoR (41.99°) and the lowest relative error (0.666%). In contrast, Series C and D resulted in higher AoR or greater variability, while Series E showed inconsistent results with a high coefficient of variation (CoV). Among all runs in the simulation, A7 was selected as the best match to the experimental AoR (41.72°), due to its low variability across trials (StDev = 2.76°) and acceptable error (0.154%), showing that it has more stable simulation behavior. While B7 also showed another good accuracy, its larger standard deviation (8.590°) made A7 the more reliable choice.

**Table 4.** Summary of Simulated AoR Results – Tree leaves

| Simulation | AoR (°) | StDev (°) | Relative Error (%) |
|---|---|---|---|
| B11 | 42.44 | 7.544 | 1.755 |
| B2 | 42.22 | 8.688 | 1.230 |
| B7 | 41.99 | 8.590 | 0.666 |
| A7 | 41.66 | 2.767 | 0.154 |

For sawdust, only one parameter group (Series F) was evaluated, containing five different sets (F1–F5) as shown in Table 5. Among them, F5 produced an AoR of 39.03°, which was virtually identical to the experimental measurement of 39.28°. This resulted in a small relative error of 0.63% and a relatively low standard deviation of 2.68°. The close agreement between simulation and experiment confirmed that the F5 configuration provided a well-calibrated representation of sawdust flow behavior, making it the preferred set for subsequent DEM analyses.

**Table 5.** Summary of Simulated AoR Results – Sawdust

| Simulation | AoR (°) | StDev (°) | Relative Error (%) |
|---|---|---|---|
| F1 | 40.47 | 7.201 | 3.027 |
| F2 | 38.27 | 5.754 | 2.581 |
| F3 | 40.27 | 2.364 | 2.521 |
| F4 | 42.65 | 7.855 | 8.569 |
| F5 | 39.039 | 2.683 | 0.631 |

**Table 6.** Summary of Simulated AoR Results – Mixture

| Simulation | AoR (°) | StDev (°) | Relative Error (%) |
|---|---|---|---|
| G4 | 39.633 | 7.256 | 1.131 |
| G6 | 40.712 | 5.870 | 1.560 |
| G9 | 39.047 | 7.913 | 2.594 |
| G10 | 41.070 | 4.681 | 2.452 |
| H2 | 39.131 | 5.638 | 2.385 |
| H9 | 40.608 | 2.198 | 1.298 |

For the mixture, two parameter series (G and H) consisting of 10 sets each. As shown in Table 6, summarize the top-performing parameter sets. G6 produces a simulated AoR of 40.71°, offering a good balance between a high AoR, moderate consistency with a low relative error of 1.56% and reasonable stability (StDev = 5.87°). While G10 (AoR = 41.07°, StDev = 4.68°) provides the highest AoR and lowest variability, its higher relative error (2.45%) made it less ideal in terms of accuracy. On the other hand, H9 provided the most accurate AoR (40.60°) with the lowest error (1.29%) and the lowest standard deviation (2.19°). Thus, considering both accuracy and stability, H9 was selected as the most reliable and practical parameter set for simulating the behavior of the biomass mixture in DEM.

## 4. CONCLUSIONS

In this study, the key simulation parameters of biomass materials such as sawdust, tree leaves, and their mixture were calibrated through angle of repose (AoR) experiments combined with DEM trial-and-error adjustments. Using the fixed funnel method, the AoR was measured as 41.66° for tree leaves (three repetitions), 39.28° for sawdust (two repetitions), and 40.08° for the mixture (two repetitions). These AoR values were then used as benchmarks to fine-tune parameters in the Hertz-Mindlin with the JKR contact model until the simulated AoR closely matched the experimental results.

For tree leaves, the best agreement was obtained with test A7, which produced an AoR of 41.72° and a small error of 0.15% with low variability. Sawdust calibration was most accurate in test F5, giving an AoR of 39.03° and an error of 0.63%. For the mixture, test H9 provided the most balanced outcome, with AoR of 40.60° and an error of 1.29%. The corresponding calibrated parameters for tree leaves were: Poisson's ratio 0.300, shear modulus 10.000 MPa, restitution 0.002, static friction 0.600, rolling friction 0.070, and JKR surface energy 0.100 J/m². Sawdust parameters were: Poisson's ratio 0.300, shear modulus 6.000 MPa, restitution 0.020, static friction 0.760, rolling friction 0.120, and JKR surface energy 0.120 J/m². For the mixture, the optimal set was Poisson's ratio 0.260, shear modulus 7.684 MPa, restitution 0.067, static friction 0.660, rolling friction 0.080, and JKR surface energy 0.098 J/m².

Although the DEM model successfully captured the overall flow characteristics of these biomass materials, it does not fully reflect the variability in cohesion caused by moisture or compaction. Furthermore, scale effects between the laboratory setup and industrial systems may also introduce deviations. The calibration in this study also relied on a trial-and-error approach rather than the design of experiments or response surface methodology. This choice was made due to computational constraints and the complexity of cohesive biomass, but it limits the ability to quantify the uncertainty and explore the parameter space.

Despite these limitations, the calibrated parameters provide a solid foundation for future DEM studies and contribute valuable insights for improving flow prediction in practical applications. They enable more accurate prediction of biomass flowability, mixing behaviour, and handling performance in a continuous mixer, which reduces the need for repeated physical trials and supports improved design and optimization of biomass processing operations.

## ACKNOWLEDGMENTS

The author sincerely thanks Dr. KAN Kuchvichea of the Road Materials Laboratory, Department of Civil Engineering, ITC, for providing the supporting structure used in the Angle of Repose experiment. His contribution was vital to the success of this study.

## REFERENCES

[1] R. R. Gupta and R. Agarwal, *Recent Technologies for Waste to Clean Energy and its Utilization*. 2023.

[2] B. Wu, "The Sustainable Technology Research on High-Efficiency Conversion and Utilization of Biomass-Based Energy," *Acad. J. Sci. Technol.*, vol. 9, no. 1, pp. 114–118, 2024, doi: 10.54097/0465fw53.

[3] N. J. Sliper, "Energy Utilization and Conversion in Modern Biomass Conversion Technologies," *J. Comput. Intell. Mater. Sci.*, vol. 2, pp. 1–11, 2024, doi: 10.53759/832x/jcims202402001.

[4] S. Swapan et al., "Combustion characteristics and behaviour of agricultural biomass: a short review," *Intech*, vol. 11, no. tourism, p. 13, 2020, [Online]. Available: https://www.intechopen.com/books/advanced-biometric-technologies/liveness-detection-in-biometrics

[5] N. Hodžić et al., "Primjenom otpadne drvne biomase i Miscanthusa do održivog sektora termoenergetike u vremenu energetske tranzicije / Sustainable Energy Sector Using Waste Woody Biomass and Miscanthus in the Energy Transition," *Energ. Ekon. Ekol.*, vol. XXV, no. 1, pp. 1–9, 2023, doi: 10.46793/eee23-1.01h.

[6] L. Carlos Ujados et al., "Bioenergy as an Environmental Alternative in Energy Systems: A Case Study," p. 1481, 2018, doi: 10.3390/proceedings2231481.

[7] Heang et al., "Experimental Investigation on Sawdust-Tree Leaves Briquette Using Fish Oil and Waste Oil As Binder," no. June 2023, 2020.

[8] J. Klinger *et al.*, "Multiscale Shear Properties and Flow Performance of Milled Woody Biomass," *Front. Energy Res.*, vol. 10, no. July, pp. 1–15, 2022, doi: 10.3389/fenrg.2022.855289.

[9] D. Barletta, R. J. Berry, S. H. Larsson, T. A. Lestander, M. Poletto, and Á. Ramírez-Gómez, "Assessment on bulk solids best practice techniques for flow characterization and storage/handling equipment design for biomass materials of different classes," *Fuel Process. Technol.*, vol. 138, pp. 540–554, 2015, doi: 10.1016/j.fuproc.2015.06.034.

[10] H. Yi et al., "Finite element modeling of biomass

hopper flow," *Front. Energy Res.*, vol. 11, no. May, pp. 1–12, 2023, doi: 10.3389/fenrg.2023.1162627.

[11] T. L. W. and D. S. Hartley, "Biomass Handling and Feeding," *Intech*, vol. 11, no. tourism, p. 21, 2018, [Online]. Available: https://www.intechopen.com/books/advanced-biometric-technologies/liveness-detection-in-biometrics

[12] A. Hamed, Y. Xia, N. Saha, J. Klinger, D. N. Lanning, and J. Dooley, "Flowability of Crumbler Rotary Shear Size-Reduced Granular Biomass: An Experiment-Informed Modeling Study on the Angle of Repose," *Front. Energy Res.*, vol. 10, no. May, pp. 1–20, 2022, doi: 10.3389/fenrg.2022.859248.

[13] J. Falk et al., "Mass flow and variability in screw feeding of biomass powders - Relations to particle and bulk properties," *Powder Technol.*, vol. 276, pp. 80–88, 2015, doi: 10.1016/j.powtec.2015.02.023.

[14] P. A. Cundall and O. D. L. Strack, "A discrete numerical model for granular assemblies," *Geotechnique*, vol. 30, no. 3, pp. 331–336, 1979, doi: 10.1680/geot.1980.30.3.331.

[15] T. De, A. Das, and J. Kumar, "On the prediction of particle collision behavior in coarse-grained and resolved systems," *Part. Sci. Technol.*, vol. 41, no. 8, pp. 1170–1184, 2023.

[16] A. Sac-Morane, M. Veveakis, and H. Rattez, "A Phase-Field Discrete Element Method to study chemo-mechanical coupling in granular materials," *Comput. Methods Appl. Mech. Eng.*, vol. 424, 2024, doi: 10.1016/j.cma.2024.116900.

[17] M. Bagheri, S. Roy, and T. Pöschel, "Discrete Element Simulations of particles interacting via capillary forces using MercuryDPM," *SoftwareX*, vol. 29, no. November 2024, p. 101987, 2025, doi: 10.1016/j.softx.2024.101987.

[18] S. Rotter, M. Dosta, and A. Düster, "Discrete element simulation of the breakage behavior of porous granules utilizing bond models," *Comput. Part. Mech.*, vol. 11, no. 1, pp. 89–103, 2024, doi: 10.1007/s40571-023-00610-0.

[19] J. Quist and M. Evertsson, "Framework for DEM Model Calibration and Validation," *Proc. 14th Eur. Symp. Comminution Classif.*, no. September, pp. 103–108, 2015.

[20] Y. Tan et al., "Automated measurement of the numerical angle of repose (aMAoR) of biomass particles in EDEM with a novel algorithm," *Powder Technol.*, vol. 388, pp. 462–473, 2021, doi: 10.1016/j.powtec.2021.04.062.

[21] M. Hofmann, "On the Complexity of Parameter Calibration in Simulation Models," *J. Def. Model. Simul. Appl. Methodol. Technol.*, vol. 2, no. 4, pp. 217–226, 2005, doi: 10.1177/154851290500200405.

[22] R. Hajivand Dastgerdi, "A Simplified Calibration Procedure for DEM Simulations of Granular Material Flow," *Materials (Basel).*, vol. 17, no. 19, 2024, doi: 10.3390/ma17194833.

[23] C. Zheng et al., *Discrete Element Modelling of Pharmaceutical Powder Handling Processes*, no. January. 2023. doi: 10.1002/9783527835935.ch7.

[24] H. M. Beakawi Al-Hashemi et al., "A review on the angle of repose of granular materials," *Powder Technol.*, vol. 330, pp. 397–417, 2018, doi: 10.1016/j.powtec.2018.02.003.

[25] G. Ma et al., "Calibration of Contact Parameters for Moist Bulk of Shotcrete Based on EDEM," *Adv. Mater. Sci. Eng.*, vol. 2022, 2022, doi: 10.1155/2022/6072303.

[26] J. Ren *et al.*, "Discrete Element Simulation Modeling Method and Parameters Calibration of Sugarcane Leaves," *Agronomy*, vol. 12, no. 8, pp. 1–21, 2022, doi: 10.3390/agronomy12081796.

[27] X. Wang et al., "Calibration of Simulation Parameters for Roasted Green Tea Based on Discrete Element Method," *Nongye Jixie Xuebao/Transactions Chinese Soc. Agric. Mach.*, vol. 55, no. 8, pp. 418–427, 2024, doi: 10.6041/j.issn.1000-1298.2024.08.039.

[28] M. Rackl et al., "Qualitative and quantitative assessment of 3D-scanned bulk solid heap data," *Powder Technol.*, vol. 321, pp. 105–118, 2017, doi: 10.1016/j.powtec.2017.08.009.

[29] J. Zhang, C. Li, Q. Niu, P. Wang, L. Wang, and H. Li, "Characterization of green peppers based on dynamic repose angle," *LWT*, vol. 180, no. November 2022, p. 114703, 2023, doi: 10.1016/j.lwt.2023.114703.

[30] M. G. Kleinhans et al., "Static and dynamic angles of repose in loose granular materials under reduced gravity," *J. Geophys. Res. Planets*, vol. 116, no. 11, pp. 1–13, 2011, doi: 10.1029/2011JE003865.

[31] L. Zhichao, "Measuring the Angle of Repose of Granular Systems," *Can. Geotech. J.*, p. 143, 2011, [Online]. Available: http://d-scholarship.pitt.edu/6401/1/MSThesisZhichaoLiu03042011.pdf

[32] D. McGlinchey, *Characterisation of Bulk Solids*. 2004.

[33] G. Xun, B. XueWei, H. HaiBo, Z. FengYu, G. YuanJuan, and W. DeSheng, "Dem Parameters Calibration of Mixed Biomass Sawdust Model With Multi-Response Indicators," *INMATEH - Agric. Eng.*, vol. 65, no. 3, pp. 183–192, 2022, doi: 10.35633/INMATEH-65-19.

[34] Z. Chik and L. E. Vallejo, "Characterization of the angle of repose of binary granular materials," *Can. Geotech. J.*, vol. 42, no. 2, pp. 683–692, 2005, doi: 10.1139/t04-118.

[35] H. N. Pitanga et al., "Interface shear strength of

geosynthetics: Evaluation and analysis of inclined plane tests," *Geotext. Geomembranes*, vol. 27, no. 6, pp. 435–446, 2009, doi: 10.1016/j.geotexmem.2009.05.003.

[36] International Standard ISO 4324, "Surface active agents - Powders and granules - Measurement of the angle of repose," vol. 1977, 1977.

[37] I. S. B. Ferreira, R. S. Peruchi, N. J. Fernandes, and P. Rotella Junior, "Measurement system analysis in angle of repose of fertilizers with distinct granulometries," *Meas. J. Int. Meas. Confed.*, vol. 170, no. May, 2021, doi: 10.1016/j.measurement.2020.108681.

[38] P. Datta and S. A. Faroughi, "Angle of repose for superquadric particles: Investigating the effects of shape parameters," *Comput. Geotech.*, vol. 165, 2024, doi: 10.1016/j.compgeo.2023.105918.

[39] M. Paulick et al., "Review on the influence of elastic particle properties on DEM simulation results," *Powder Technol.*, vol. 283, pp. 66–76, 2015, doi: 10.1016/j.powtec.2015.03.040.

[40] W. Fang, X. Wang, D. Han, and X. Chen, "Review of Material Parameter Calibration Method," *Agric.*, vol. 12, no. 5, 2022, doi: 10.3390/agriculture12050706.

[41] C. Coetzee, "A Johnson-Kendall-Roberts (JKR) Contact Model, Implementation in PFC," no. 03 December, 2020, doi: 10.13140/RG.2.2.21772.54404.

[42] J. Hærvig *et al.*, "On the adhesive JKR contact and rolling models for reduced particle stiffness discrete element simulations," *Powder Technol.*, vol. 319, pp. 472–482, 2017, doi: 10.1016/j.powtec.2017.07.006.

[43] M. J. Carr, W. Chen, K. Williams, and A. Katterfeld, "Comparative investigation on modelling wet and sticky material behaviours with a simplified JKR cohesion model and liquid bridging cohesion model in DEM," *ICBMH 2016 - 12th Int. Conf. Bulk Mater. Storage, Handl. Transp. Proc.*, pp. 40–49, 2016.

[44] N. N. Mohsenin, "Physical properties of plant and animial materials. Vol. 1. Structure, physical characterisitics and mechanical properties.," 1970.

[45] Z. Yan et al., "Discrete element modelling (DEM) input parameters: understanding their impact on model predictions using statistical analysis," *Comput. Part. Mech.*, vol. 2, no. 3, pp. 283–299, 2015, doi: 10.1007/s40571-015-0056-5.

[46] J. Lei *et al.*, "Discrete element contact parameters measurement and calibration of sugarcane leaves based on RSM-PSO," *BioResources*, vol. 18, no. 3, p. 4994, 2023.

[47] Jiang et al., "Design and experiment on spiral impurity cleaning device for profile modeling residual plastic film collector," 2019.

[48] L. Chen *et al.*, "Calibration of discrete meta-parameters of bamboo flour based on magnitude analysis and BP neural network," *PLoS One*, vol. 19, no. 10, 2024, doi: 10.1371/journal.pone.0308019.

[49] R. Mistry, C. Dalal, and T. Soni, "International Journal of Advanced Research in Electrical, Electronics and Instrumentation Engineering Determination of Angle of Repose of Pharmaceutical Materials Based On Image Processing Using Labview," *Int. J. Adv. Res. Electr. Electron. Instrum. Eng.*, pp. 1125–1131, 2017, doi: 10.15662/IJAREEIE.2017.0603020.

[50] M. D. Kurkuri, C. Randall, and D. Losic, "New method of measuring the angle of repose of hard wheat grain," in *Chemeca 2012: Quality of life through chemical engineering: 23-26 September 2012, Wellington, New Zealand*, Engineers Australia Barton, ACT, 2012, pp. 1814–1821.